# RSC Advances

## RSC Advances

www.rsc.org/advances

This is an *Accepted Manuscript*, which has been through the Royal Society of Chemistry peer review process and has been accepted for publication.

*Accepted Manuscripts* are published online shortly after acceptance, before technical editing, formatting and proof reading. Using this free service, authors can make their results available to the community, in citable form, before we publish the edited article. This *Accepted Manuscript* will be replaced by the edited, formatted and paginated article as soon as this is available.

You can find more information about *Accepted Manuscripts* in the **Information for Authors**.

Please note that technical editing may introduce minor changes to the text and/or graphics, which may alter content. The journal's standard **Terms & Conditions** and the **Ethical guidelines** still apply. In no event shall the Royal Society of Chemistry be held responsible for any errors or omissions in this *Accepted Manuscript* or any consequences arising from the use of any information it contains.

ROYAL SOCIETY OF CHEMISTRY

www.rsc.org/advances

# Journal Name

ROYAL SOCIETY OF CHEMISTRY

## ARTICLE TYPE

# Influence of dye-TiO$_2$ interface on DSSC performance: a theoretical exploration with ruthenium dye[†]

Ling-Jun He,[a] Jie Chen,[a] Fu-Quan Bai,[a] Ran Jia,[a] Jian Wang,[*a] and Hong-Xing Zhang[*a]

Density functional theory (DFT) and time-dependent DFT (TD-DFT) approaches were applied to explore the influence of dye-TiO$_2$ interface on DSSC performance by taking heteroleptic Ru(II) dye as an example. Our analysis was based on the interpretation of the dye-TiO$_2$ geometry, electronic structure, and light harvesting and utilization. The results indicate that the alkaline electrolyte is necessary if the solar cell was fabricated with Ru dye coordinated with 2-5-bis(N-pyrazolyl)pyridine and bipyridine ligands. Higher average thermodynamic driving force of **a**@(TiO$_2$)$_5$(OH) structure ensures the better electron injection ability. Proper modification of the acceptor ligand (4-carboxyl-pyridine fragment) not only expands the absorption coverage, but also improves the ability to capture more photons within effective absorption bands. Despite the absorption coverage is further expanded within the **c**@(TiO$_2$)$_5$(OH) geometry, the relatively weaker molar absorption coefficient declines the light harvesting capability. The extra absorption bands in the lower energy region indicates more photons will be captured in **b**@(TiO$_2$)$_5$(OH) structure, therefore leading to a higher short-circuit current density. Our results elucidate the effect of dye-TiO$_2$ interface on DSSC performance and supply a promising way to estimate and screen out the possible candidate for DSSCs application.

## 1 Introduction

Due to an urgent requirement for the energy, accompanied by the increasing in environmental pollution and the consumption of fossil fuels, seeking for alternative pollution-free and renewable energy have been taken on the agenda. Dye-sensitized solar cells (DSSCs) attract attention globally because of their high photoelectric conversion efficiency, pollution-free, and bargain price since the breakthrough work reported by O'Regan and Grätzel in 1991.[1] In recent years, DSSCs gradually replace the status of the traditional solar cells, and also it has turned into a promising alternative to the conventional amorphous silicon and other inorganic semiconductor-based photovoltaic devices,[2–4] the low current conversion slows down its further application, this is especially true when compared with other solid solar cell, such as the perovskite solar cell, which attains a conversion efficiency as high as 20%. From the point of view DSSC operating mechanism, the overall efficiency of DSSC is controlled by the following: a) the light harvest; b) electron injection; c) electron collection on the dye-semiconductor interface; d) dye regeneration.[3,5,6] Abundant efforts have been committed to overcome the bottleneck of DSSC

by covering one or more of the above aspects. Recently, the experimental investigations and theoretical design of Ru(II) center sensitizers have already made great processes either by extending $\pi$-conjugated[7], evaluating the role of ancillary ligands[8], or exploring the connection style of dye on semiconductor[9]. Philippopoulos et al.[10] synthesized and evaluated a series of heteroleptic Ru(II) sensitizers and finally concluded that the photovoltaic performance depends remarkably on the number of COOH functional groups. Our previous contribution[11] indicates not only the number of COOH group, but also the substituent position on the electron donor or acceptor ligand determines the light harvest and charge injection efficiency, thus affect the overall efficiency of DSSC. However, all these conclusions are based on electronic properties of single dye molecule without considering other facts such as dye-semiconductor interface, due to the computing capacity limit at that moment.

Additionally, the study on different substitution site for the auxiliary anchoring group is rarely mentioned. Considering the direct connection for the anchor group with the semiconductor, it is a crucial element for the dye-TiO$_2$ interface to determine whether the DSSCs are high-efficiency or not. Generally speaking, the interface between dye and semiconductor plays a vital role in reaching higher photoelectric conversion efficiency. It is because the interface determines the position where the electron injection happens and where the charge transfer starts. And plenty

[a] International Joint Research Laboratory of Nano-Micro Architecture Chemistry, Institute of Theoretical Chemistry, Jilin University, 130023, Changchun, China. E-mail: zhanghx@jlu.edu.cn; abbott.cn@gmail.com
[†] Electronic Supplementary Information (ESI) available: [details of any supplementary information available should be included here]. See DOI: 10.1039/b000000x/
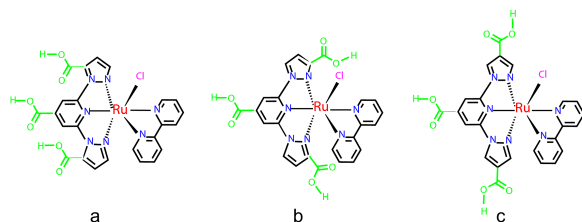
RSC Advances Accepted Manuscript

**Fig. 1** Schematic representation of dye **a**, **b**, and **c**.

attempts also have been devoted to investigate the interaction between dye and $TiO_2$ surface and the charge transfer mechanism upon it.[12–28] In current contribution, we push the previous study further by considering the dye-semiconductor interface to explore how the dye-$TiO_2$ interface structure affects the efficiency of DSSC.

## 2 Computational details

### 2.1 DFT and TDDFT calculations

In this work, all the calculations were performed by the Gaussian 09 program package.[29] All ground state geometries of dye and dye@$TiO_2$ were fully optimized with density functional theory (DFT) method at B3LYP[30]/LanL2DZ; 6-31G(d) level of theory, which has been successfully applied for theoretical investigation of ruthenium dyes.[11,31,32] Then at the same level of theory the harmonic vibrational frequencies were computed in order to check the nature of the stationary points, namely to check if all the frequencies were real. The electronic properties of dye and dye@$TiO_2$ in excited states were explored by time-dependent density functional theory (TD-DFT) approach. In order to select a proper functional to estimate the excitation energy, we have compared the results of excited state based on the B3LYP, CAM-B3LYP,[33] and LC-BLYP[34] with LanL2DZ and 6-31G(d) hybrid basis sets. All the informations for the discussion were collected in ESI†. Solvent effects were considered by using the Polarizable Continuum Model (PCM) of SCRF procedure for dimethyldisulfide (DMSO).

### 2.2 The efficiency of DSSC

At any given wavelength $\lambda$, the incident photon to current efficiency ($\eta_{IPCE}(\lambda)$) is a function of the light harvesting efficiency ($\eta_{LHE}(\lambda)$), and the efficiency of charge injection ($\varphi_{inject}$) from the electronic excited state to the conduction band of $TiO_2$, combining with the charge collection efficiency ($\eta_c$). (If the dye is different in main body, but similar in the dye-$TiO_2$ interface, the $\eta_c$ can be considered to be the same.) Thus the $\eta_{IPEC}(\lambda)$ can be expressed as:

$$\eta_{IPCE}(\lambda) = \varphi_{inject} \cdot \eta_{LHE}(\lambda) \cdot \eta_c \qquad (1)$$

here, $\varphi_{inject}$ depends on the thermodynamic driving force ($D$) of electrons injecting from the excited states of dye to the semiconductor substrate.

$$\varphi_{inject} \propto D \qquad (2)$$

Obviously, accompanied by the increase of $D$, the efficiency of charge injection would be higher, assuming injection takes place at or near Frank-Condon region. $D$ can be expressed as[35]:

$$D = E^* - E_{cb} = E^0 + \Delta E - E_{cb} \qquad (3)$$

where,

- $E^*$, the redox potential in excited state;

- $E^0$, the redox potential in ground state, which can be calculated in accordance with the Nernst equation;[11]

- $\Delta E$, the vertical excitation energy which can be obtained from TD-DFT calculation;

- $E_{cb}$, the conduction band edge of $TiO_2$.

The light harvesting efficiency at the given wavelength $\lambda$ can be calculated as[36,37]:

$$\eta_{LHE}(\lambda) = 1 - 10^{-\Gamma \sigma(\lambda)} \qquad (4)$$

where,

- $\Gamma$, the surface loading of sensitizers (mol/cm$^2$) grafted onto semiconductor. In current work, $\Gamma$ is set to $1.6 \times 10^{-7}$ mol/cm$^2$ according to the previous publication on Ru-based dyes[10];

- $\sigma(\lambda)$, the molecular absorption cross-section (cm$^2$/mol). It is a function related to the molar absorption coefficient ($\varepsilon(\lambda)$) and can be expressed as following[36,38]:

$$\sigma(\lambda) = 1000 \cdot \varepsilon(\lambda) \qquad (5)$$

## 3 Results and discussion

### 3.1 Geometry of dye-$TiO_2$ interface

As illustrated in Fig. 1, for clarity, we label the three Ru(II) complexes $[Ru(bpp\text{-}1)(bpy)Cl]^+$, $[Ru(bpp\text{-}2)(bpy)Cl]^+$, and $[Ru(bpp\text{-}3)(bpy)Cl]^+$ (bpp=2,6-bis(N-pyrazolyl)pyridine, bpp-1=1,1'-(4-carboxypyridine-2,6-diyl)bis(1-H-pyrazole-5-carboxylic acid), bpp-2=1,1'-(4-carboxypyridine-2,6-diyl)bis(1-H-pyrazole-3-carboxylic acid), bpp-3=1,1'-(4-carboxypyridine-2,6-diyl)bis(1-H-pyrazole-4-carboxylic acid), bpy=2-2'-bipyridine) as **a**, **b**, and **c**, respectively. Accordingly, we label the corresponding dye-semiconductor structure as **a**@$(TiO_2)_5$, **b**@$(TiO_2)_5$, and **c**@$(TiO_2)_5$, referring to Fig. 2.

The $TiO_2$ surfaces are generated from the optimized bulk geometry exposing the most thermodynamically stable surface: (101) in the case of anatase. In general, nanoparticle surfaces apply the anatase (101) surface to simulate the semiconductor, because this surface has smaller surface energy and a high efficiency for DSSC.[39,40] In current work, anatase $Ti_5O_2OH_{22}$ (101) models from crystal structures is adopted as the surface of $TiO_2$ film, in this model, the covalent bond of O atoms are saturated by extra H atoms, giving out the $Ti_5O_2OH_{22}$ semiconductor model. This method not only maintains bond-orientation in crystal but also averts the confusions of multiplicity and charge in the whole
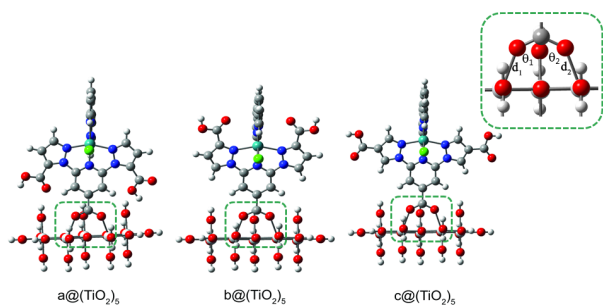
**Fig. 2** Optimized dye@$(TiO_2)_5$ structures calculated on B3LYP/LanL2DZ; 6-31G(d) level.

system. Additionally, these Ti atoms can be divided into two types: One is five-coordinated and another is six-coordinated. The five-coordinated Ti atoms are located at anatase (101) surface, which used for adsorption site. While the six-coordinated Ti atoms cut out from the $TiO_2$ crystal bulk. The calculated bond lengths $d_1/d_2$ between two carboxylate oxygens and connected titanium atoms on the $TiO_2$ film of the $a@(TiO_2)_5$, $b@(TiO_2)_5$, and $c@(TiO_2)_5$ system are: 2.137/2.298 Å, 2.193/2.247 Å, and 2.192/2.255 Å, respectively, which are comparable with the Ti−O bond length in dye-$TiO_2$ interface calculated with larger cluster models, such as 2.12/2.10 Å with $(TiO_2)_{256}$ model[41], 2.08/2.08 Å with $(TiO_2)_{36}$ model[42], and 2.216/2.166 Å, 2.121/2.172 Å with $(TiO_2)_{28}$ model[43]. It indicates that such small scale models could be sufficient to simulate the real physical properties of $TiO_2$, and this strategy has been successfully applied in previous study[32,44–46]. Additionally, the angles of $\theta_1$ and $\theta_2$ as shown in Fig. 2 are 129.7°/131.4°, 134.2°/134.6°, and 134.3°/134.5° in $a@(TiO_2)_5$, $b@(TiO_2)_5$, and $c@(TiO_2)_5$, respectively. From the point of view of bond length and angle, it can be concluded that the three dye-$TiO_2$ interfaces are similar in geometry though the auxiliary anchoring groups are attached to different sites. Meanwhile, the dye-$TiO_2$ interface is where the excited charge be captured or collected by the semiconductor. Therefore, the nearly same dye-$TiO_2$ interface geometry would lead to essentially same charge collection efficiency ($\eta_c$) among **a**, **b**, and **c**.

While in a real DSSC system, the dye-$TiO_2$ interface may not only be steeped in electrolyte, but also be affected by temperature and other environmental factors. As a result, the hydrogen atoms in the anchoring group of dye molecular may be dissociated. We have calculated all possible dye-$TiO_2$ structures which may arise from dehydrogenation process. The calculation indicates there is no significant changes in bond length and angle on the dye-$TiO_2$ interface. From this point of view, we may speculate that, whether dehydrogenation or not has little affect on the geometry of dye-$TiO_2$ interface.

### 3.2 Electronic structure properties

The appropriate energy level layout of dye is one of the prerequisite for fast charge transfer. For DSSC system, the lowest unoccupied molecular orbital (LUMO) should be higher in energy than the lower edge of conduction band of $TiO_2$ ($E_{LUMO}$ > -4.0

**Table 1** The HOMO and LUMO energy levels (in eV) for all dyes and dye-$TiO_2$s.

| dye | a | a@$(TiO_2)_5$(2H) | a@$(TiO_2)_5$(1H) | a@$(TiO_2)_5$(OH) |
|---|---|---|---|---|
| $E_{LUMO}$ | -3.10 | -4.06 | -3.79 | -3.48 |
| $E_{HOMO}$ | -6.08 | -6.33 | -5.88 | -5.44 |
| dye | b | b@$(TiO_2)_5$(2H) | b@$(TiO_2)_5$(1H) | b@$(TiO_2)_5$(OH) |
| $E_{LUMO}$ | -3.11 | -4.08 | -3.87 | -3.69 |
| $E_{HOMO}$ | -6.04 | -6.25 | -5.68 | -5.21 |
| dye | c | c@$(TiO_2)_5$(2H) | c@$(TiO_2)_5$(1H) | c@$(TiO_2)_5$(OH) |
| $E_{LUMO}$ | -3.06 | -4.04 | -3.91 | -3.77 |
| $E_{HOMO}$ | -6.06 | -6.26 | -5.71 | -5.49 |

**Table 2** The composition of HOMO and LUMO for all isolate dyes.

| dye | orbital | composition | | | | |
|---|---|---|---|---|---|---|
| | | Ru | Cl | bpy | cpyra[1] | cpy[2] |
| **a** | LUMO | 0.08 | 0 | 0 | 0.31 | 0.60 |
| | HOMO | 0.64 | 0.16 | 0.13 | 0.07 | 0 |
| **b** | LUMO | 0.08 | 0 | 0 | 0.22 | 0.68 |
| | HOMO | 0.66 | 0.16 | 0.12 | 0.06 | 0 |
| **c** | LUMO | 0.08 | 0 | 0 | 0.12 | 0.79 |
| | HOMO | 0.66 | 0.17 | 0.12 | 0.06 | 0 |

[1] Refers to 1-H-pyrazole-3-carboxylic acid or something like.
[2] Refers to 4-carboxyl-pyridine.

eV), this could guarantee the efficient electron injection from the excited dye into the semiconductor substrate. While the highest occupied molecular orbital (HOMO) should lie between the upper edge of valence band of $TiO_2$, and the redox potential of $I^-/I_3^-$ (in current case, -4.60 eV > $E_{HOMO}$ > -7.20 eV), which could guarantee the efficient dye regeneration that the excited dyes could get electron from the electrolyte fleetly. The calculated HOMO and LUMO energy values are tabulated in Table 1. The results indicate that the dye itself fully match the above-mentioned energy level requirement, namely, there are possibilities that dye **a**, **b**, and **c** could play as sensitizer in DSSC.

While the dye itself alone does not construct a real DSSC. The sensitiser should be attached to $TiO_2$ and soaked in electrolyte at least. The energy level of all possible dye-$TiO_2$ structures are listed in Table 1. The calculation reveals that the HOMO and LUMO energy levels are pushed downwards to a even lower position by attaching $TiO_2$ fragment, resulting in that dye **a**, **b**, and **c** might not be capable of DSSC application from the point of view energy level. However, if the electrolyte can be tuned into alkaline environment, the energy value of LUMO would be higher than -4.0 eV, see the last two rows in Table 1, which means that the alkaline electrolyte solution is necessary when building DSSC with dye **a**, **b**, or **c**, otherwise the cell may not work. Therefore, in the following sections, we only talk about the dye-$TiO_2$ structures in the forms of $a@(TiO_2)_5$(OH), $b@(TiO_2)_5$(OH), $c@(TiO_2)_5$(OH), that's to say, all the hydrogens in carboxyl groups are dissociated.

As known to us, the open-circuit photovoltage ($V_{oc}$) is also a crucial parameter to evaluate the efficiency of DSSC device. Proper charge population improves $V_{oc}$. The correlation of charge populations and experimental $V_{oc}$ indicates that more charges
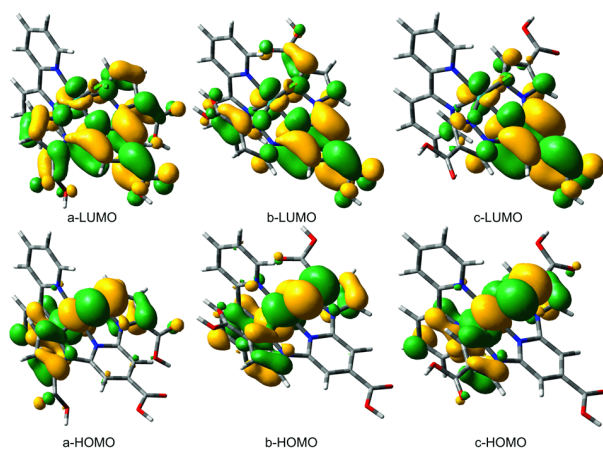
**Fig. 3** The HOMO and LUMO diagrams of dye **a**, **b**, and **c** at PCM-B3LYP/Lanl2DZ; 6-31G(d) level of theory.



**Fig. 4** The HOMO and LUMO diagrams of dye@$(TiO_2)_5$ at PCM-B3LYP/Lanl2DZ; 6-31G(d) level of theory.

populated in acceptor groups results in larger $V_{oc}$[47]. The molecular orbital composition reveals that more than 90% of the charge would populate on the bpp ligand in **a**, **b**, and **c**. Especially, as the change of substituent positions of −COOH group on pyrazole fragment in **a**, **b**, and **c**, more and more charges (from 60% in **a**, to 68% in **b**, and 79% in **c**, see Table 2 and Fig. 3) populates on 4-carboxyl-pyridine fragment (abbreviated as, cpy), which acts as a charge acceptor fragment and a tunnel to transfer charge from dye to conduction band of semiconductor. Therefore, it can be prognosticated that $V_{oc}$ could be further improved if the cell is fabricated with dye **c**.

Moreover, in order to better understand the nature of charge transfer process, we present several important orbitals in Fig. 4. As shown in Fig. 4, in current case, the HOMO is primarily populated on the dyes, whereas the LUMO is delocalized on the $TiO_2$. This kind of electronic structure is consistent with dye@$TiO_2$ electronic character in DSSC application. In other words, the electronic property of dye@$TiO_2$ system can be also described by the smaller $(TiO_2)_5$ cluster model.

### 3.3 Light harvesting and utilization

The DSSCs now used to turn sunlight into electricity can only absorb and use a small fraction of that light, and which means that an abundant of solar energy goes untapped. Harvesting more energy from sunlight requires a broadband absorption which can cover as much as possible the solar spectral irradiance in the visible and near infrared region. In this work, the fitted Gaussian type absorption curves of dye-$TiO_2$ are illustrated in Fig. 5 and the corresponding character vertical excitations calculated from TD-DFT are listed in Table 4. The half-width at half height is set to 0.1 eV in gaussview, so that the character molar extinction value can be compared with the experimental values. At first glance, the molar absorption coefficient decreases but the absorption bands are widened in **b** and **c** as compared with that of **a**. But one can not take it for granted that all the absorption bands in lower energy bands really contribute to photon to electricity transfer process. According to the operation mechanism of
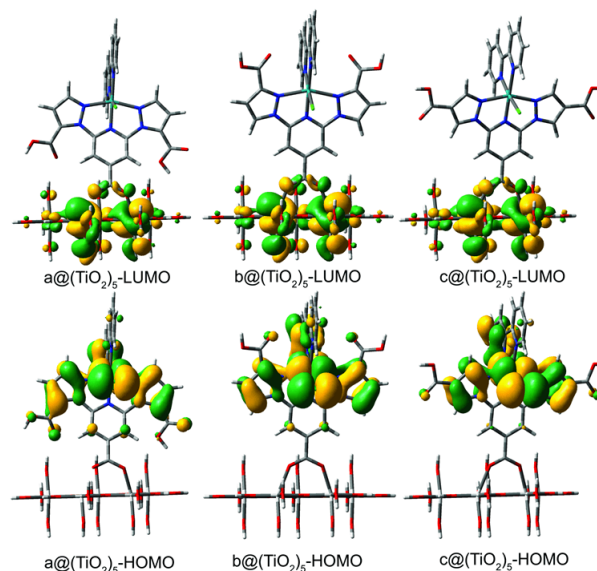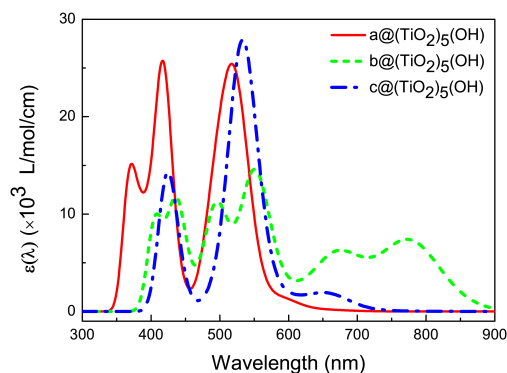


**Fig. 5** The absorption spectrum at B3LYP/LanL2DZ; 6-31G(d) level in DMSO solvent.

**Table 3** Calculated redox potential ($E^0$, in V) and Gibbs free energy ($\Delta G_{sol}$, in au).

| dye@$(TiO_2)_5$ | a@$(TiO_2)_5$(OH) | b@$(TiO_2)_5$(OH) | c@$(TiO_2)_5$(OH) |
|---|---|---|---|
| $\Delta G_{sol}$ | 0.187 | 0.178 | 0.197 |
| $E^0$ | -5.083 | -4.852 | -5.365 |

**Table 4** Selected calculated excitation energy ($\Delta E$, eV), wavelength ($\lambda$, nm), oscillator strength ($f$), driving force ($D$, eV) for all the dye@$(TiO_2)_5$ complex.

| dye@$(TiO_2)_5$ | Excitation(\|CI coeff.\|) [1] | $\Delta E$ | $D$ | $\lambda$ | $f$ |
|---|---|---|---|---|---|
| a@$(TiO_2)_5$(OH) | H→L+9(0.63) | 2.35 | 1.27 | 527 | 0.1056 |
| | H-1→L+6(0.71) | 2.52 | 1.44 | 492 | 0.0691 |
| | H-1→L+16(0.45) | 3.32 | 2.24 | 374 | 0.0375 |
| | H→L+18(0.77) | 3.41 | 2.33 | 364 | 0.0146 |
| b@$(TiO_2)_5$(OH) | H-1→L+1(0.94) | 1.59 | 0.74 | 779 | 0.0484 |
| | H-3→L+1(0.74) | 1.86 | 1.01 | 666 | 0.0209 |
| | H-1→L+6(0.88) | 2.24 | 1.39 | 553 | 0.0903 |
| | H-3→L+6(0.88) | 2.50 | 1.65 | 496 | 0.0740 |
| | H→L+16(0.63) | 2.84 | 1.99 | 437 | 0.0674 |
| | H-13→L+1(0.89) | 3.06 | 2.21 | 406 | 0.0371 |
| c@$(TiO_2)_5$(OH) | H-5→L+1(0.95) | 1.89 | 0.53 | 656 | 0.0127 |
| | H-5→L+5(0.85) | 2.25 | 0.89 | 552 | 0.0196 |
| | H-5→L+6(0.78) | 2.33 | 0.97 | 533 | 0.1852 |
| | H-3→L+14(0.35) | 2.92 | 1.56 | 425 | 0.0365 |
| | H→L+17(0.44) | 2.98 | 1.62 | 416 | 0.0256 |

[1] H represents for HOMO, L represents for LUMO

DSSC, to guarantee a beneficial charge transfer process, on the one hand, the value of the redox potential of dye in excited state, $E^*$, should be higher in value than the conduction band of semiconductor; on the other hand, the energetics of the excited states should be high enough to provide a thermodynamic driving force ($D$) to accomplish charge injection (namely, larger $D$ is better). If the vertical excitations which contribute the absorption band satisfy the above-mentioned requirements, then the exact absorption band is the so-called valid absorption band. And only the valid absorption band has the opportunity to contribute the final photon to electricity conversion efficiency.

The redox potential of **a**, **b**, and **c** in ground state is calculated to be -5.08 V, -4.85 V, and -5.36 V, which is 1.08 V, 0.85 V, and 1.37 V below the conduction band of $TiO_2$, respectively, as shown in Table 3. Therefore, the vertical excitation energy should not less than 1.08 eV in **a**, otherwise the final excited state would not be energetic enough to transfer the electron to the conduction band of $TiO_2$. As reported in Table 4, the main excitation energy are greater than 1.08 eV, therefore all absorption bands of **a** are valid. Similarly, the absorption bands of **b** and **c** in current case are all effective. From this point of view, it can deem that the electronic structure of dye-$TiO_2$ interface will be changed obviously by proper modification of the acceptor segment. In addition, according to Eq. 2, the average driving force of **a**, **b**, and **c** goes in the order of **a** (1.82 ) > **b** (1.49) > **c** (1.11), indicating that **a** would be optimal in the performance of charge injection.

However, the weak molar absorption coefficient may make **c** a flash in the pan. There's another character we should take into account, the $\eta_{LHE}(\lambda)$. We have shown the $\eta_{LHE}(\lambda)$ profile of
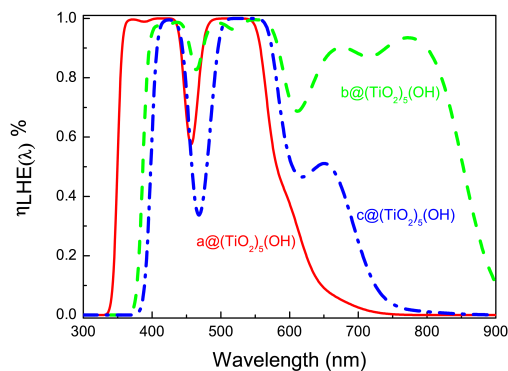


**Fig. 6** The plot of the $\eta_{LHE}(\lambda)$ curves for all strucures.

each dye in Fig. 6, it is obvious that the **b**@$(TiO_2)_5$(OH) has wider cover range and higher $\eta_{LHE}(\lambda)$ at 600 nm - 900 nm than others. But only $\eta_{LHE}(\lambda)$ does not make any sense, because the photon number varies with the change of wavelength.

The DSSC is used to convert the exited photons into electricity current. If more photons were captured, there would be more electrons to be excited, thereby resulting in more charges being injected into the conduction band of $TiO_2$, and finally improves the short-circuit current density ($J_{sc}$) of solar cell. $J_{sc}$ is related to the integral photon flux density ($\Phi(\lambda)$) in the whole absorption coverage. The $\Phi(\lambda)$ is defined as the number of photons per second per unit area and per unit wavelength, it can be evaluated by following equation at given wavelength ($\lambda$),

$$\Phi(\lambda) = \frac{P(\lambda)}{E} \qquad (6)$$

thus, the total photon number per second per unit area within the whole spectrum coverage can be calculated by the following equation:

$$\int \Phi(\lambda) \cdot d\lambda = \int \frac{P(\lambda)}{E} \cdot d\lambda \qquad (7)$$

where,

- $P(\lambda)$, the spectral power density in $W \cdot m^{-2} \cdot m^{-1}$;

- $E$, the energy of photon at the wavelength of light ($\lambda$).

The $E$ can be expressed as:

$$E = \frac{h \cdot c}{\lambda} \qquad (8)$$

where,

- $h$, the Planck's constant, $6.626 \times 10^{-34}$ J $\cdot$ s;

- $c$, the speed of light, $3.0 \times 10^8$ m/s.

Additionally, the maximal photon generated current ($J_{ph}$) can be expressed as:

$$J_{ph} = q \int \Phi(\lambda) \cdot d\lambda \qquad (9)$$

where,

- $q$, the elementary charge, $1.6 \times 10^{-19}$ C.

here, the flow of electric charge across a surface per second per unit area in whole spectrum that is equivalent to the maximum short circuit density ($J_{sc}^{max}$) the cell can produced.

On the one hand, the experimental determined sun irradiance is too complicated to be expressed within a simple formula; on the other hand, the spectral irradiance of sun is well approximated by the emission of a blackbody with temperature of about 5778 K[48]. Hence, the power density at the given wavelength can be rewritten as:

$$P(\lambda) = (\frac{R}{D})^2 \frac{2\pi h c^2}{\lambda^5 (e^{\frac{hc}{\kappa \lambda T}} - 1)} \tag{10}$$

where,

- $R$, the radius of sun, $0.695 \times 10^9$ m;

- $D$, the distance from sun to earth, $1.496 \times 10^{11}$ m;

- $\kappa$, Boltzmann's constant, $1.3806488 \times 10^{-23}$ J/K;

- $T$, temperature of blackbody. Here, $T = 5778$ K.

In fact, the radiation absorbed by dyes is not absolutely complete, with the consideration of the practical condition, we introduce $\eta_{LHE}(\lambda)$ for obtaining the actual absorption. With Eq. 6 and Eq. 10, the exact part of photon flux density ($\Phi(\lambda)$) generated by dyes per second per unit area at the given wavelength ($\lambda$) can be rewritten as ($\lambda$ in m):

$$
\begin{aligned}
\Phi(\lambda) &= (\frac{R}{D})^2 \eta_{LHE}(\lambda) \frac{2\pi c}{\lambda^4 (e^{\frac{hc}{\kappa \lambda T}} - 1)} \\
&= 40682.5 \times \frac{1 - 10^{-\Gamma\sigma(\lambda)}}{\lambda^4 (e^{\frac{2.49 \times 10^{-6}}{\lambda}} - 1)}
\end{aligned}
\tag{11}
$$

Finally, the $J_{ph}$ for $\mathbf{a}@(TiO_2)(OH)$, $\mathbf{b}@(TiO_2)(OH)$, $\mathbf{c}@(TiO_2)(OH)$ can be obtained according to the Eq. 9. The $J_{ph}$ which can be generated by $\mathbf{a}@(TiO_2)(OH)$, $\mathbf{b}@(TiO_2)(OH)$, and $\mathbf{c}@(TiO_2)(OH)$ within the absorption coverage 300 - 900 nm is calculated to be 15.1 mA/cm$^2$, 31.2 mA/cm$^2$, and 16.0 mA/cm$^2$, respectively. As the above mentioned, due to the flow of electric charge across a surface per second per unit area in whole spectrum that is equivalent of short circuit density ($J_{sc}^{max}$), therefore, it can deem that the $\mathbf{b}@(TiO_2)(OH)$ structure can generate the largest $J_{sc}^{max}$. That is to say, the $J_{sc}^{max}$ of the solar cell will be further improved if the cell is fabricated with $\mathbf{b}$ as compared with the other two.

## 4 Conclusion

DFT and TD-DFT approaches were applied to explore the influence of interface between dye and semiconductor on DSSC performance. In this work, the dye-TiO$_2$ structures with (TiO$_2$)$_5$ cluster model were investigated theoretically. Though the dye-TiO$_2$ structure remains as it was when $H^+$ dissociates from the $-$COOH anchoring group due to the change of pH in electrolyte environment, the LUMO of dye-TiO$_2$ structure was pushed to a higher energy level, which is advantageous for rapid charge transfer process. More charge would populate on the charge acceptor ligand (4-carboxyl-pyridine fragment) if the auxiliary anchoring group on pyrazole fragment are located far away from the Ru(II)

core. Higher average thermodynamic driving force indicates that $\mathbf{a}@(TiO_2)_5(OH)$ structure is more conductive to electron injection. Though the absorption coverage is further expanded within the $\mathbf{c}@(TiO_2)_5(OH)$ geometry, the relatively weaker molar absorption coefficient hinders the improvement of light utilization. With the help of solar radiation's power density, our calculation reveals that larger $J_{sc}^{max}$ is obtained within the absorption coverage 300 – 900 nm in $\mathbf{b}@(TiO_2)_5(OH)$ structure, namely higher short-circuit current density could be expected if the solar cell is fabricated with dye $\mathbf{b}$ in alkaline electrolyte. In a nutshell, we hope that this theoretical investigation work will be helpful for improving and designing new sensitizers in DSSC, so as to satisfy with the vast requirement of DSSC territory.

## Acknowledgements

## References

1 B. O'Regan and M. Grätzel, *Nature*, 1991, **353**, 737–740.

2 M. Grätzel, *Nature*, 2001, **414**, 338–344.

3 A. Hagfeldt, G. Boschloo, L. C. Sun, L. Kloo and H. Pettersson, *Chemical Reviews*, 2010, **110**, 6595–6663.

4 G. Boschloo and A. Hagfeldt, *Accounts of Chemical Research*, 2009, **42**, 1819–1826.

5 M. Grätzel, *Journal of Photochemistry and Photobiology C: Photochemistry Reviews*, 2003, **4**, 145 – 153.

6 M. Law, L. E. Greene, J. C. Johnson, R. Saykally and P. Yang, *Nat Mater*, 2005, **4**, 455–459.

7 H. Ozawa, K. Fukushima, A. Urayama and H. Arakawa, *Inorganic Chemistry*, 2015, **54**, 8887–8889.

8 T. Jella, M. Srikanth, R. Bolligarla, Y. Soujanya, S. P. Singh and L. Giribabu, *Dalton Trans.*, 2015, **44**, 14697–14706.

9 J. Chen, J. Wang, F. Q. Bai, L. Hao, Q. J. Pan and H. X. Zhang, *Dyes and Pigments*, 2013, **99**, 201–208.

10 A. I. Philippopoulos, A. Terzis, C. P. Raptopoulou, V. J. Catalano and P. Falaras, *European Journal of Inorganic Chemistry*, 2007, 5633–5644.

11 J. Wang, F.-Q. Bai, B.-H. Xia, L. Feng, H.-X. Zhang and Q.-J. Pan, *Phys. Chem. Chem. Phys.*, 2011, **13**, 2206–2213.

12 C. Barolo, M. K. Nazeeruddin, S. Fantacci, D. Di Censo, P. Comte, P. Liska, G. Viscardi, P. Quagliotto, F. De Angelis, S. Ito and M. Grätzel, *Inorganic Chemistry*, 2006, **45**, 4642–4653.

13 P. Qin, H. J. Zhu, T. Edvinsson, G. Boschloo, A. Hagfeldt and L. C. Sun, *Journal of the American Chemical Society*, 2008, **130**, 8570–8571.

14 M. Nilsing, S. Lunell, P. Persson and L. Ojamae, *Surface Science*, 2005, **582**, 49–60.

15 M. Nilsing, P. Persson and L. Ojamae, *Chemical Physics Letters*, 2005, **415**, 375–380.

16  P. Persson and M. J. Lundqvist, *Journal of Physical Chemistry B*, 2005, **109**, 11918–11924.

17  M. J. Lundqvist, M. Nilsing, S. Lunell, B. Akermark and P. Persson, *Journal of Physical Chemistry B*, 2006, **110**, 20513–20525.

18  P. Persson, M. J. Lundqvist, R. Ernstorfer, W. A. Goddard and F. Willig, *Journal of Chemical Theory and Computation*, 2006, **2**, 441–451.

19  M. Nilsing, P. Persson, S. Lunell and L. Ojamae, *Journal of Physical Chemistry C*, 2007, **111**, 12116–12123.

20  H. Wolpher, S. Sinha, J. X. Pan, A. Johansson, M. J. Lundqvist, P. Persson, R. Lomoth, J. Bergquist, L. C. Sun, V. Sundstrom, B. Akermark and T. Polivka, *Inorganic Chemistry*, 2007, **46**, 638–651.

21  S. Ghosh, G. K. Chaitanya, K. Bhanuprakash, M. K. Nazeeruddin, M. Grätzel and P. Y. Reddy, *Inorganic Chemistry*, 2006, **45**, 7600–7611.

22  M. K. Nazeeruddin, Q. Wang, L. Cevey, V. Aranyos, P. Liska, E. Figgemeier, C. Klein, N. Hirata, S. Koops, S. A. Haque, J. R. Durrant, A. Hagfeldt, A. B. P. Lever and M. Grätzel, *Inorganic Chemistry*, 2006, **45**, 787–797.

23  M. S. Lowry and S. Bernhard, *Chemistry-a European Journal*, 2006, **12**, 7970–7977.

24  J. R. Li, M. Nilsing, I. Kondov, H. B. Wang, P. Persson, S. Lunell and M. Thoss, *Journal of Physical Chemistry C*, 2008, **112**, 12326–12333.

25  D. P. Hagberg, T. Marinado, K. M. Karlsson, K. Nonomura, P. Qin, G. Boschloo, T. Brinck, A. Hagfeldt and L. Sun, *Journal of Organic Chemistry*, 2007, **72**, 9550–9556.

26  H. Qin, S. Wenger, M. Xu, F. Gao, X. Jing, P. Wang, S. M. Zakeeruddin and M. Grätzel, *Journal of the American Chemical Society*, 2008, **130**, 9202–9203.

27  W. H. Howie, F. Claeyssens, H. Miura and L. M. Peter, *Journal of the American Chemical Society*, 2008, **130**, 1367–1375.

28  H. N. Tian, X. C. Yang, R. K. Chen, R. Zhang, A. Hagfeldt and L. C. Sunt, *Journal of Physical Chemistry C*, 2008, **112**, 11023–11033.

29  M. Frisch, G. Trucks, H. B. Schlegel, G. Scuseria, M. Robb, J. Cheeseman, G. Scalmani, V. Barone, B. Mennucci and G. Petersson, *Wallingford, CT*, 2009, **19**, 227–238.

30  C. Lee, W. Yang and R. G. Parr, *Phys. Rev. B*, 1988, **37**, 785–789.

31  L. Salassa, C. Garino, G. Salassa, R. Gobetto and C. Nervi, *Journal of the American Chemical Society*, 2008, **130**, 9590–9597.

32  K. Syres, A. Thomas, F. Bondino, M. Malvestuto and M. Grätzel, *Langmuir*, 2010, **26**, 14548–14555.

33  T. Yanai, D. P. Tew and N. C. Handy, *Chemical Physics Letters*, 2004, **393**, 51–57.

34  Y. Tawada, T. Tsuneda, S. Yanagisawa, T. Yanai and K. Hirao, *The Journal of Chemical Physics*, 2004, **120**, 8425–8433.

35  A. Furube, R. Katoh, T. Yoshihara, K. Hara, S. Murata, H. Arakawa and M. Tachiya, *The Journal of Physical Chemistry B*, 2004, **108**, 12583–12592.

36  M. K. Nazeeruddin, A. Kay, I. Rodicio, R. Humphry-Baker, E. Mueller, P. Liska, N. Vlachopoulos and M. Graetzel, *Journal of the American Chemical Society*, 1993, **115**, 6382–6390.

37  J. Zhang, J.-Z. Zhang, H.-B. Li, Y. Wu, Y. Geng and Z.-M. Su, *Phys. Chem. Chem. Phys.*, 2014, **16**, 24994–25003.

38  M. Grätzel, *Inorganic Chemistry*, 2005, **44**, 6841–6851.

39  U. Diebold, N. Ruzycki, G. Herman and A. Selloni, *Catalysis Today*, 2003, **85**, 93 – 100.

40  M. Lazzeri, A. Vittadini and A. Selloni, *Phys. Rev. B*, 2001, **63**, 155409.

41  P.-P. Sun, Q.-S. Li, L.-N. Yang, Z.-Z. Sun and Z.-S. Li, *Phys. Chem. Chem. Phys.*, 2014, **16**, 21827–21837.

42  N. Santhanamoorthi, K.-H. Lai, F. Taufany and J.-C. Jiang, *Journal of Power Sources*, 2013, **242**, 464 – 471.

43  K. Chaitanya, X.-H. Ju and B. M. Heron, *RSC Adv.*, 2015, **5**, 3978–3998.

44  K. Syres, A. Thomas, F. Bondino, M. Malvestuto and M. Grätzel, *Langmuir*, 2010, **26**, 14548–14555.

45  M. Xie, J. Wang, H.-Q. Xia, F.-Q. Bai, R. Jia, J.-G. Rim and H.-X. Zhang, *RSC Adv.*, 2015, **5**, 33653–33665.

46  M. Xie, J. Chen, J. Wang, C.-P. Kong, F.-Q. Bai, R. Jia and H.-X. Zhang, *Theoretical Chemistry Accounts*, 2015, **134**, NULL.

47  C.-R. Zhang, L. Liu, J.-W. Zhe, N.-Z. Jin, Y. Ma, L.-H. Yuan, M.-L. Zhang, Y.-Z. Wu, Z.-J. Liu and H.-S. Chen, *International journal of molecular sciences*, 2013, **14**, 5461–5481.

48  G.-s. WU, T. WEN, Z.-w. WANG and S.-p. LIU, *Telecom Power Technology*, 2013, **1**, 007.